

Hepta/octa cyanomolybdates with Fe²⁺: influence of the valence state of Mo on the magnetic behavior

Amandeep K. Sra,^a Guillaume Rombaut,^b Frédéric Lahitête,^b Stéphane Golhen,^{c†} Lahcène Ouahab,^c Corine Mathonière,^{*b} J. V. Yakhmi^a and (the late) Olivier Kahn^b

^a Novel Materials and Structural Chemistry Division, Bhabha Atomic Research Center, Mumbai 400085, India

^b Laboratoire des Sciences Moléculaires, Institut de Chimie de la Matière Condensée de Bordeaux, UPR CNRS No. 9048, F-33608 Pessac, France. E-mail: mathon@icmcb.u-bordeaux.fr

^c Laboratoire de Chimie du Solide et Inorganique Moléculaire, UMR CNRS No 6511, Université de Rennes 1, F-35042 Rennes, France. E-mail: golhen@univ-rennes1.fr

Received (in Strasbourg, France) 6th June 2000, Accepted 19th August 2000

First published as an Advance Article on the web 25th October 2000

Two Fe^{II}-based molybdenum polycyanides, Fe₂[Mo^{III}(CN)₇] · 8H₂O and [Fe₂(H₂O)₄][Mo^{IV}(CN)₈] · 4H₂O, have been synthesized. The compound [Fe₂(H₂O)₄][Mo^{IV}(CN)₈] · 4H₂O crystallizes in the tetragonal system, space group I422. There are two molybdenum sites in a distorted square antiprism arrangement, each site being surrounded by eight CN–Fe linkages. The distorted octahedral iron site is formed by four NC–Mo linkages and two water molecules in apical positions. The structure is three-dimensional and highly symmetrical. The magnetic characteristics of these two compounds were compared. Fe₂[Mo^{III}(CN)₇] · 8H₂O orders below 65 K as a ferrimagnet, but [Fe₂(H₂O)₄][Mo^{IV}(CN)₈] · 4H₂O shows no evidence of long-range magnetic order, obviously due to the contribution of the diamagnetic Mo^{IV} which suppresses the propagation of magnetic interaction between adjacent iron(II) ions through CN bridges. The results are discussed in the light of the single-crystal structural features of [Fe₂(H₂O)₄][Mo^{IV}(CN)₈] · 4H₂O.

The design of molecule-based magnets from molecular precursors is an area of current interest. The cyano bridge is an attractive candidate for this since it can mediate strong anti-ferromagnetic or ferromagnetic interactions, as evidenced in the case of Prussian Blue analogues {PBA; general formula A_k[B(CN)₆]_x · xH₂O where A and B are transition metal ions with different oxidation and spin states}.^{1,2} However, these hexacyanometalates often suffer from inherent disorder among different cationic sites, making it difficult to grow the single crystals required to perform detailed physical measurements. Besides, their highly symmetric face-centred cubic structure³ does not offer much scope for the study of anisotropy in magnetic properties. This situation led us to look for novel cyano-based bimetallic extended lattices with lower symmetry than that of the PBAs. Towards this, we focussed on employing the heptacyanide anion [Mo^{III}(CN)₇]^{4–} as a precursor because its pentagonal bipyramidal coordination sphere is incompatible with a cubic lattice. Moreover, the [Mo^{III}(CN)₇]^{4–} chromophore is a low-spin species (*S*_{Mo} = 1/2), and the *g* tensor associated with the ground Kramers doublet is very anisotropic.⁴ Two- and three-dimensional compounds have been synthesized by the reaction of manganese(II) ions with [Mo(CN)₇]^{4–}. The structure and magnetic properties were investigated in detail in our groups, including the magnetic anisotropy and magnetic phase diagrams.^{5–8} The nature of the low spin Mo³⁺ interaction with high spin Mn²⁺ through the Mo^{III}–C–N–Mn^{II} bridges is ferromagnetic, irrespective of the structural details, with moderate values for the Curie temperatures (*T*_c = 51 K). This temperature is shifted to 65 K in related dehydrated compounds.⁶ Recently, however, we observed a much reduced

ordering temperature (*T*_c only 3 K) in [Mn^{II}L]₆[Mo^{III}(CN)₇]₆ · 19.5H₂O, L being the macrocyclic ligand 2,13-dimethyl-3,6,9,12,18-pentaazabicyclo[12.3.1]octadeca-1(18),2,12,14,16-pentaene, which was attributed to the existence of Mo as diamagnetic Mo⁴⁺ along certain CN bridges, in addition to paramagnetic Mo³⁺.⁹ Therefore, it is of interest to examine the role of Mo⁴⁺ ions exclusively in the propagation of spin–spin interactions in 3d-based Mo–polycyanide compounds.

In view of this we undertook the synthesis of two Fe^{II}-based Mo-polycyanides, namely Fe₂[Mo^{III}(CN)₇] · 8H₂O and [Fe₂(H₂O)₄][Mo^{IV}(CN)₈] · 4H₂O and report their magnetic behavior in this paper. The synthesis of the latter compound has been described previously, but without much detail about structural or magnetic characteristics, in view of the non-availability of single crystals.¹⁰ Single crystals of [Fe₂(H₂O)₄][Mo^{IV}(CN)₈] · 4H₂O suitable for X-ray diffraction have been obtained and the structure solved. The magnetic behaviour of these two compounds has been investigated. Polycrystalline Fe₂[Mo^{III}(CN)₇] · 8H₂O orders below 65 K as a ferrimagnet and [Fe₂(H₂O)₄][Mo^{IV}(CN)₈] · 4H₂O behaves as a paramagnet down to fairly low temperatures. For this latter compound, we discuss the influence of Mo⁴⁺ ions on the Fe^{II}–Fe^{II} spin–spin interaction in the light of its structural features.

Experimental

Synthesis

All manipulations were performed under a well ventilated hood due to the toxicity of the cyano chemistry. K₄[Mo(CN)₇] · 2H₂O and K₄[Mo(CN)₈] · 2H₂O were synthesized as described in the literature.⁴

† Author for enquiries relating to the crystallographic studies.

Fe₂[Mo(CN)₇]·8H₂O. Powders and solvents were first degassed; 1.32 mmol (0.598 g) of K₄[Mo(CN)₇]·2H₂O dissolved in about 50 ml of degassed water were slowly added under N₂ to 2.64 mmol (0.731 g) of FeSO₄·7H₂O dissolved in 100 ml of degassed water. A blue precipitate appeared which was filtered off, washed several times with degassed water, and then dried under a current of N₂. Since the compound is air sensitive it was stored under N₂ in sealed tubes. It is poorly crystalline and all attempts to obtain single crystals were unsuccessful. Calc. For C₇H₁₆Fe₂MoN₇O₈: C, 15.75; H, 3.02; Fe, 20.92; Mo, 17.97; N, 18.37. Found: C, 16.13; H, 2.92; Fe, 20.40; Mo, 18.60; N, 18.22%. On the basis of the chemical analysis the compound was formulated as Fe₂[Mo(CN)₇]·8H₂O.

[Fe₂(H₂O)₄][Mo(CN)₈]·4H₂O. This compound was prepared using the procedure described in ref. 10. Yellow octahedral single crystals were obtained by slow diffusion in water, in an H-shaped tube, of two 5 ml aqueous solutions containing 0.1 mmol of K₄[Mo(CN)₈]·2H₂O and 0.2 mmol of FeSO₄·4H₂O, respectively.

IR spectra

IR spectra were recorded with a Perkin-Elmer Paragon 1000 spectrometer from KBr pellets in the 4000–400 cm^{−1} range.

Structure determination

For the determination of the crystal structure of [Fe₂(H₂O)₄][Mo(CN)₈]·4H₂O, data were collected on an Enraf Nonius CAD4 diffractometer. Data reduction and correction was performed with MOLEN.¹¹ Lorentz polarisation and semi-empirical absorption corrections (ψ -scan method)¹² were applied to intensities for all data. Scattering factors and corrections for anomalous dispersion were taken from ref. 13. The structure was solved by direct methods using SHELXS-86 and structure refinement was performed with SHELXL 97¹⁴ by least squares against F_o^2 using 73 parameters. Refinement of variables with anisotropic thermal parameters, with 1337 observed reflections having $I \geq 2\sigma(I)$, gave the refined structural parameters listed in Tables 1 and 2.

CCDC reference number 440/214. See <http://www.rsc.org/suppdata/nj/b0/b004566g/> for crystallographic files in .cif format.

Table 1 Crystal data and structure refinement of [Fe₂(H₂O)₄][Mo(CN)₈]·4H₂O

Empirical formula	C ₈ H ₁₆ Fe ₂ MoN ₈ O ₈
Formula weight	559.93
T/K	293(2)
$\lambda/\text{\AA}$	0.71073
Crystal system	Tetragonal
Space group	I422
$a/\text{\AA}$	11.809(2)
$c/\text{\AA}$	13.108(2)
$V/\text{\AA}^3$	1828.1(6)
Z	4
μ/mm^{-1}	2.297
Final $R1, wR2$ indices [$I > 2\sigma(I)$] (all data)	0.0555, 0.1414 0.0782, 0.1482

Magnetic measurements

Magnetic data for both compounds were recorded using a Quantum Design MPMS-5S magnetometer working both in the dc and ac modes in the temperature range 2–300 K under an applied field up to 50 kOe. The compound Fe₂[Mo(CN)₇]·8H₂O is air sensitive, and its magnetic investigations were carried out on a polycrystalline sample placed in a quartz tube sealed under vacuum.

Results and discussion

Infrared analyses

The IR spectrum of Fe₂[Mo(CN)₇]·8H₂O shows a broad strong band ν_{CN} at 2123 cm^{−1} with a shoulder at 2074 cm^{−1}. These two peaks are at higher wavenumbers than the peaks observed for K₄[Mo(CN)₇]·2H₂O at 2067 and 2035 cm^{−1}, confirming the bridging nature of the cyano groups. Note that the presence of two peaks instead of one accounts for the low local symmetry of the molybdenum(III) site. The spectra and the chemical composition of Fe₂[Mo(CN)₇]·8H₂O are close to those of the three-dimensional Mn²⁺ compounds of formula [Mn₂(H₂O)₅][Mo(CN)₇]· n H₂O.^{6,7,15} The IR spectra of these Mn²⁺ compounds show a broad strong band ν_{CN} at 2118 cm^{−1} with a shoulder at 2079 cm^{−1}. However, due to the non-availability of single crystals or any powder X-ray diffraction data suitable for analysis, it is difficult to obtain any structural information for this Fe²⁺ compound through analogy because for the Mn²⁺ compound two pseudo polymorphs exist, namely the α phase ($n = 4$) and the

Table 2 Selected bond lengths (Å) and angles (°) for Fe₂(H₂O)₄[Mo(CN)₈]·4H₂O^a

Mo(1)–C(1)	2.128(15)	Fe(1)–N(1)	2.222(10)
Fe(1)–O(2)	2.110(12)	Mo(2)–C(2)	2.153(14)
Fe(1)–N(2)	2.114(11)	C(1)–N(1)	1.192(18)
Fe(1)–O(1)	2.177(13)	C(2)–N(2)	1.212(18)
C(1)–Mo(1)–C(1) ⁱ	111.3(8)	C(2)–Mo(2)–C(2) ⁱ	115.7(7)
C(1)–Mo(1)–C(1) ⁱⁱ	83.9(10)	C(2)–Mo(2)–C(2) ^v	73.6(3)
C(1)–Mo(1)–C(1) ⁱⁱⁱ	138.0(8)	C(2)–Mo(2)–C(2) ^{vii}	73.6(3)
C(1)–Mo(1)–C(1) ^{iv}	77.6(7)	C(2)–Mo(2)–C(2) ^{viii}	139.0(12)
C(1)–Mo(1)–C(1) ^v	71.4(4)	C(2)–Mo(2)–C(2) ^{ix}	79.1(8)
C(1)–Mo(1)–C(1) ^{vi}	148.3(9)	C(2)–Mo(2)–C(2) ^j	145.3(11)
C(1)–Mo(1)–C(1) ^{vii}	71.4(4)	C(2)–Mo(2)–C(2) ^j	75.1(10)
N(2)–Fe(1)–N(2) ^{viii}	161.9(6)	N(1)–C(1)–Mo(1)	168.5(14)
N(2)–Fe(1)–N(1) ^{viii}	91.4(3)	C(1)–N(1)–Fe(1)	146.0(12)
N(2)–Fe(1)–N(1)	90.4(3)	N(2)–C(2)–Mo(2)	158.7(16)
N(1)–Fe(1)–N(1) ^{viii}	168.2(5)	C(2)–N(2)–Fe(1)	158.5(13)
Fe(1)··Fe(1) ^{vii}	6.039(1)	Fe(1)··Fe(1) ⁱⁱⁱ	9.716(2)
Fe(1)··Fe(1) ^x	6.558(3)	Fe(1)··Fe(1) ^{xi}	10.143(3)
Fe(1)··Fe(1) ^{iv}	6.795(2)	Fe(1)··Fe(1) ^{vi}	10.615(2)
Fe(1)··Fe(1) ⁱⁱ	8.029(2)		

^a Symmetry transformations used to generate equivalent atoms: $i - x, -y, z$; $ii - x, y, -z + 1$; $iii x, -y, -z + 1$; $iv y, x, -z + 1$; $v -y, x, z$; $vi -y, -x, -z + 1$; $vii y, -x, z$; $viii -y + \frac{1}{2}, -x + \frac{1}{2}, -z + \frac{1}{2}$; $ix -x, y, -z$; $x -x, 1 - y, z$; $xi 1 - x, -y, z$.

β phase ($n = 4.75$). In these the local environments of the metal sites are similar, but the three-dimensional organisations are different.^{4–7} As the number of water molecules is different in the iron compound, we may expect somewhat different three-dimensional organization.

The IR spectrum of $[\text{Fe}_2(\text{H}_2\text{O})_4][\text{Mo}(\text{CN})_8] \cdot 4\text{H}_2\text{O}$ shows a single broad strong ν_{CN} peak at 2134 cm^{-1} which is at higher wavenumber than the several sharper peaks observed for $\text{K}_4[\text{Mo}(\text{CN})_8] \cdot 2\text{H}_2\text{O}$ at 2102, 2124 and 2127 cm^{-1} , confirming the bridging nature of the cyano groups.

Crystal structure of $[\text{Fe}_2(\text{H}_2\text{O})_4][\text{Mo}^{\text{IV}}(\text{CN})_8] \cdot 4\text{H}_2\text{O}$

The single crystal structure reveals that the compound contains three metal sites: two Mo (0 0 0) and (0 0 1/2) in the intersection of a twofold and fourfold axis and one Fe ($x, 1/2 - x, 1/4$) localised on a twofold axis (Fig. 1) yielding one Mo and two Fe atoms per unit cell. Furthermore, four coordinated and four uncoordinated water molecules are present in the unit cell. The three oxygen sites (O1, O2, O3) are localised on a general position. Both O1 and O2 are bonded to Fe1, but, due to the localisation of Fe1 on a twofold axis, these two atoms have a statistical occupancy factor of 0.5. The third oxygen atom has an occupancy factor of 1.0, generating the four uncoordinated water molecules. The organisation is highly symmetrical and three-dimensional. Each Mo atom is bonded to eight Fe atoms through a cyano bridge: four Fe–N–C fragments are in the (1 1 0) plane and four others in the perpendicular (1 $\bar{1}$ 0) plane (Fig. 2). The Fe atom has somewhat distorted octahedral surroundings (Fig. 3). Each Fe atom is bonded to four N–C–Mo fragments in the (1 1 0) or (1 $\bar{1}$ 0) planes and two water molecules in apical positions. All the cyano groups are bridging and are involved in coordination to adjacent Fe^{2+} ions. Each Mo1 and Mo2 site is surrounded by eight C–N–Fe linkages, with a coordination

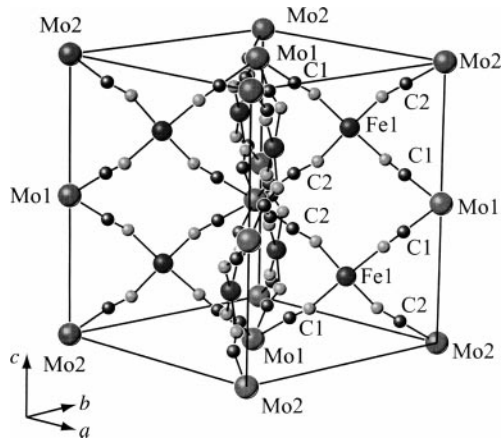


Fig. 1 Structure of the $[\text{Fe}_2(\text{H}_2\text{O})_4][\text{Mo}(\text{CN})_8] \cdot 4\text{H}_2\text{O}$ compound.

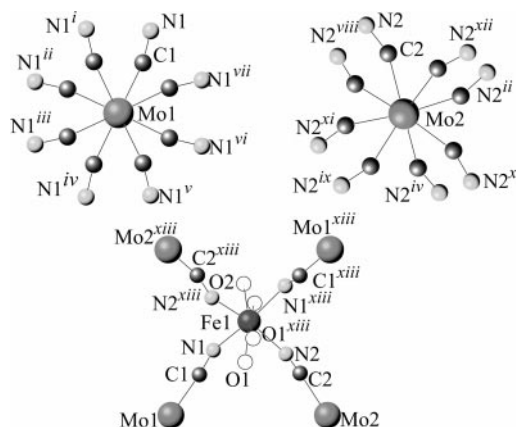


Fig. 2 Local structure of the molybdenum and iron sites.

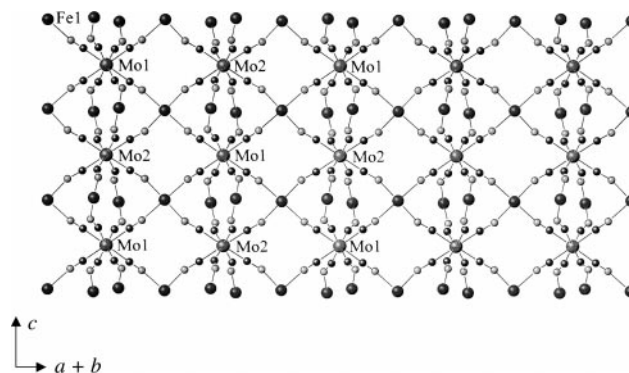


Fig. 3 Structure of $[\text{Fe}_2(\text{H}_2\text{O})_4][\text{Mo}(\text{CN})_8] \cdot 4\text{H}_2\text{O}$ viewed in the (1 1 0) plane.

reminiscent of a square antiprism (Fig. 3). The Mo1–C1 and Mo2–C2 bond lengths are equal to 2.128(15) and 2.153(14) Å. These distances are slightly lower than those observed in other polymetallic $\text{Mo}(\text{CN})_8$ based compounds.^{9,16,17} The Fe1–N1 and Fe1–N2 bond lengths are equal to 2.222(10) and 2.114(11) Å. The Mo1–C1–N1 and Mo2–C2–N2 bond angles are 168.5(14) and 158.7(16)°; the Fe1–N1–C1 and Fe1–N2–C2 angles 146.0(12) and 158.5(13)° respectively.

Magnetic properties

In this section we will first discuss $\text{Fe}_2[\text{Mo}^{\text{III}}(\text{CN})_7] \cdot 8\text{H}_2\text{O}$, which is a magnet with $T_c = 65\text{ K}$, and then $[\text{Fe}_2(\text{H}_2\text{O})_4][\text{Mo}^{\text{IV}}(\text{CN})_8] \cdot 4\text{H}_2\text{O}$, which shows no long-range magnetic ordering above 2 K.

$\text{Fe}_2[\text{Mo}^{\text{III}}(\text{CN})_7] \cdot 8\text{H}_2\text{O}$. The $\chi_m T$ vs. T plot for $\text{Fe}_2[\text{Mo}(\text{CN})_7] \cdot 8\text{H}_2\text{O}$ obtained under a 1000 Oe field is shown in Fig. 4, χ_m being the molar magnetic susceptibility and T the temperature. The $\chi_m T$ value at room temperature is $6.1\text{ emu K mol}^{-1}$ which is consistent with the Curie value of $6.4\text{ emu K mol}^{-1}$ for non-interacting spin-only moments $S(\text{Mo}^{3+}) = 1/2$, $S(\text{Fe}^{2+}) = 2$ and $g = 2$. The small difference is explained by the poor approximation of the spin-only moment for Fe^{2+} due to the spin–orbit coupling. As T is lowered, $\chi_m T$ decreases very smoothly, and reaches a minimum value around 120 K with $\chi_m T = 5.86\text{ emu K mol}^{-1}$. Upon further cooling $\chi_m T$ increased rapidly, reaching a sharp maximum of 14 emu K mol^{-1} at about 56 K and then below

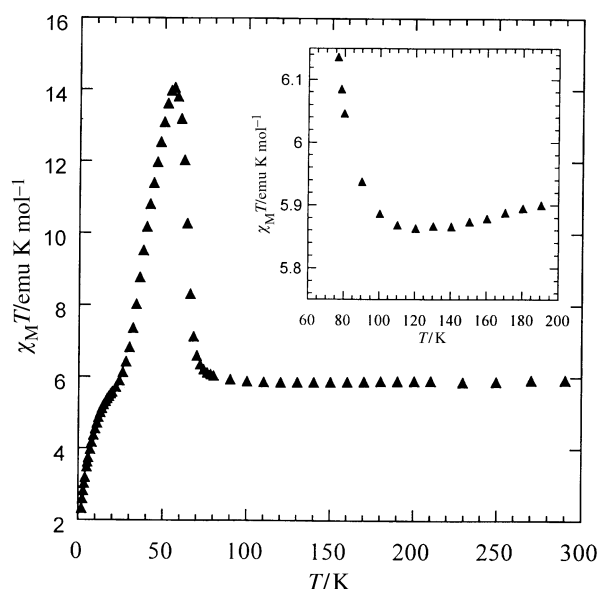


Fig. 4 Temperature dependence of $\chi_m T$ for $\text{Fe}_2[\text{Mo}(\text{CN})_7] \cdot 8\text{H}_2\text{O}$ at an applied field of 1000 Oe.

this temperature decreased, reaching a value of $2.33 \text{ emu K mol}^{-1}$ at 2 K. The minimum in the $\chi_m T$ vs. T curve indicates a ferrimagnetic behavior with a $\text{Mo}^{\text{III}}\text{--Fe}^{\text{II}}$ antiferromagnetic interaction. The low-temperature data (56–20 K) suggest that the compound exhibits a long-range magnetic ordering but the sudden drop in the $\chi_m T$ plot upon cooling the sample below 20 K is probably due to saturation effects.

To confirm the long-range magnetic ordering, the field-cooled magnetisation (FCM) and remnant magnetisation (REM) curves were recorded and are displayed in Fig. 5. The FCM curve recorded while cooling the sample under a 10 Oe field shows a break at about 65 K and a sharp increase as the temperature was lowered below 65 K, confirming the onset of ordering at this temperature. The REM curve obtained on turning the field off at 2 K and then warming the sample in zero field is typical of a magnet. The remnant magnetisation vanishes at around 65 K. Finally, the zero-field cooled magnetisation (ZFCM) was measured by cooling the sample to 2 K under 10 Oe, and recording the data while warming the sample under the applied field. The ZFCM plot shows a break at 65 K, as expected.

The ordering temperature, T_c , was also confirmed by the thermal dependence of the ac magnetic responses. Both the in-phase, χ' , and out-of-phase, χ'' , components of ac magnetic susceptibilities were recorded in the 2–80 K temperature range and the data between 40 and 80 K are shown in Fig. 6. χ' showed a sharp rise when the sample was cooled below 70 K, yielding a sharp peak at 65 K, confirming the onset of magnetic ordering at this temperature. A small broad hump observed in the χ'' plot under zero applied field conditions confirms the long range ordering, leading to a net magnetic moment and a spontaneous magnetisation below 65 K. Below 20 K an increase in χ' was observed (not represented). This may be indicative of yet another unidentified phase.

As mentioned in the Experimental, the compound is air sensitive. The secondary phase may result from a partial oxidation of $\text{Mo}^{3+}(S = 1/2)$ in $\text{Mo}^{4+}(S = 0)$. This oxidation reaction is assumed very limited, because the magnetic properties observed are not compatible with a significant amount of diamagnetic molybdenum, sites.

The magnetisation vs. field curve for this sample was recorded at 2 K. It is S-shaped with virtually no width of the hysteresis loop. The magnetisation value at 2 K under the

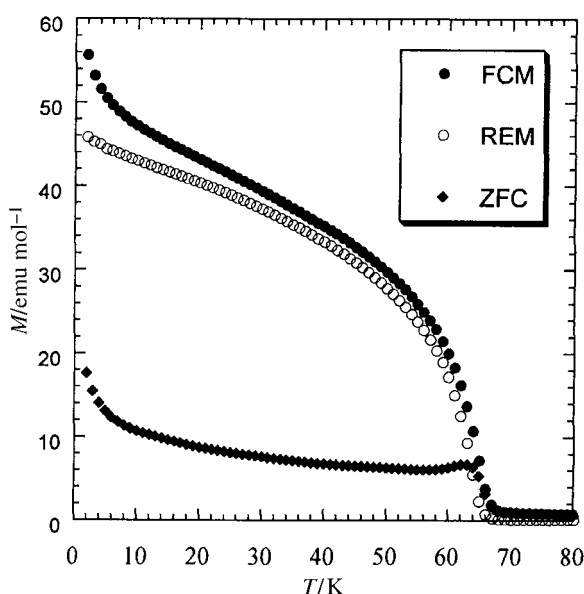


Fig. 5 FCM, ZFCM and REM magnetisation plots for $\text{Fe}_2[\text{Mo}(\text{CN})_7] \cdot 8\text{H}_2\text{O}$.

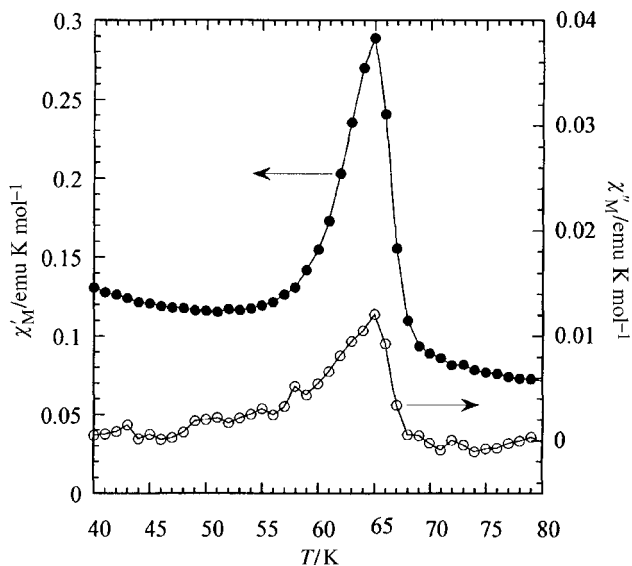


Fig. 6 The in-phase χ' and out-of-phase χ'' components of the ac susceptibility for $\text{Fe}_2[\text{Mo}(\text{CN})_7] \cdot 8\text{H}_2\text{O}$.

maximum applied field of $\pm 50 \text{ kOe}$ was $\pm 2.84 N\mu_B$, whereas the saturation magnetization value expected for $S_T = 3.5$ [presuming an antiferromagnetic coupling of two low-spin $\text{Fe}^{2+}(S = 2)$ ions and one $\text{Mo}^{3+}(S = 1/2)$ ion] is $7 N\mu_B$. The applied field of 50 kOe was not able to align the moments in the powder sample completely along the direction of the field. The origin of such a difference between measured and experimental saturation values is not clear, but may be explained partly by anisotropy caused by the spin–orbit coupling.

The high value of T_c (65 K) for $\text{Fe}_2[\text{Mo}(\text{CN})_7] \cdot 8\text{H}_2\text{O}$ is another indication of the three-dimensional organisation of the structure of this molecule-based magnet. However, due to the lack of structural details, a detailed comparison of its magnetic behavior with those recorded for the two phases of $[\text{Mn}_2(\text{H}_2\text{O})_5][\text{Mo}(\text{CN})_7] \cdot n\text{H}_2\text{O}$ is not appropriate. The T_c value for $\text{Fe}_2[\text{Mo}(\text{CN})_7] \cdot 8\text{H}_2\text{O}$ is higher than that recorded at 51 K for the α and β phases of $[\text{Mn}_2(\text{H}_2\text{O})_5][\text{Mo}(\text{CN})_7] \cdot n\text{H}_2\text{O}$, but is the same as that of the related dehydrated phases. The most interesting difference between the iron and manganese phases is the antiferromagnetic interaction between Fe^{2+} and Mo^{3+} ions through the cyanide bridge. The mechanism of the ferromagnetic interaction between Mn^{2+} and Mo^{3+} ions has not yet been clarified. In the compound described in this paper the antiferromagnetic interaction arises probably from non-zero overlap between magnetic orbitals of Fe^{2+} and Mo^{3+} ions.

$[\text{Fe}_2(\text{H}_2\text{O})_4][\text{Mo}^{\text{IV}}(\text{CN})_8] \cdot 4\text{H}_2\text{O}$. The $\chi_m T$ vs. T plot for $[\text{Fe}_2(\text{H}_2\text{O})_4][\text{Mo}(\text{CN})_8] \cdot 4\text{H}_2\text{O}$ is shown in Fig. 7. It was recorded under an applied field of 500 Oe. The $\chi_m T$ value at room temperature is $5.99 \text{ emu K mol}^{-1}$ which corresponds to the calculated spin-only value of 6 emu K mol^{-1} for two $S = 2 \text{ Fe}^{2+}$ ions, since Mo^{4+} is diamagnetic. The decrease in $\chi_m T$ at low temperature may have two main origins: spin–orbit coupling of Fe^{2+} and the presence of weak antiferromagnetic coupling between the Fe^{2+} ions. For this three-dimensional magnetic lattice, to the best of our knowledge, no theoretical model exists taking into account both spin–orbit coupling and weak antiferromagnetic coupling.

However, we tentatively tried to interpret the magnetic data as follows. The structure indicates a nearly octahedral geometry around Fe^{2+} . The electronic ground state term is $^5T_{2g}$ with orbital ($L = 2$) and spin ($S = 2$) contributions. For strictly octahedral symmetry, the orbital contribution is not quenched and we can consider only the zero-field splitting

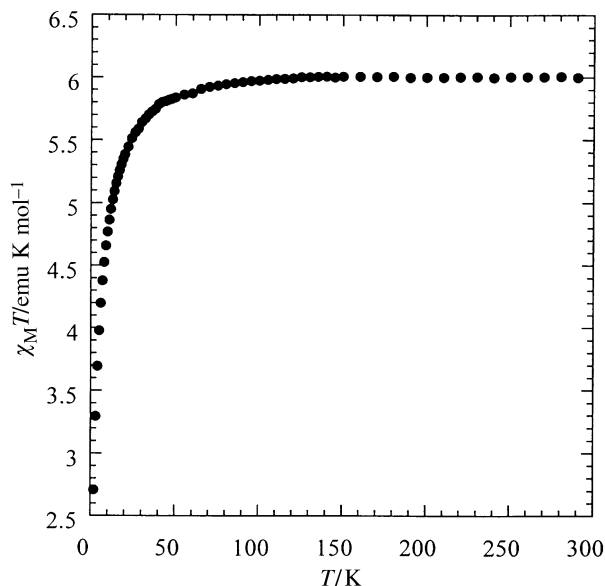


Fig. 7 Temperature dependence of $\chi_m T$ for $[\text{Fe}_2(\text{H}_2\text{O})_4][\text{Mo}(\text{CN})_8] \cdot 4\text{H}_2\text{O}$ at an applied field of 500 Oe.

(ZFS) of the $S = 2$ spin state. Then with only ZFS of Fe^{2+} , it is possible to fit the temperature dependence of the $\chi_m T$ curve. However the obtained D value ($|D| = 9.5 \text{ cm}^{-1}$) is clearly too large for such a slightly distorted octahedral Fe^{2+} site. This suggests that a weak antiferromagnetic exchange is operative. Then neglecting the ZFS of Fe^{2+} , the magnetic properties obey a Curie–Weiss law $\chi_m = C/(T - \theta)$ with a Weiss constant $\theta = -3 \text{ K}$. This negative value for θ is probably overestimated since no ZFS is taken into account here. A similar compound of formula $[\text{Mn}_2(\text{H}_2\text{O})_4][\text{Mo}(\text{CN})_8] \cdot 4\text{H}_2\text{O}$ has been prepared where the ZFS of Mn^{2+} may be neglected and the magnetic properties were interpreted with a Curie–Weiss law and $\theta = -2 \text{ K}$. We conclude that the fall of $\chi_m T$ upon cooling $[\text{Fe}_2(\text{H}_2\text{O})_4][\text{Mo}(\text{CN})_8] \cdot 4\text{H}_2\text{O}$ points to a rather weak ZFS of Fe^{2+} and a more important $\text{Fe}^{\text{II}}\text{--Fe}^{\text{II}}$ antiferromagnetic interaction in this compound at low temperatures, with no indication of the onset of long-range magnetic ordering. Since the $[\text{Fe}_2(\text{H}_2\text{O})_4][\text{Mo}(\text{CN})_8] \cdot 4\text{H}_2\text{O}$ compound is a three-dimensional structure, the interaction parameter J can be estimated with molecular-field theory. The relation between J and θ is $\theta = zJS(S + 1)/3k$ with z being the number of magnetic metal ions, S the spin value and k the Boltzmann constant. For our compound, J has been estimated at -0.13 cm^{-1} with $z = 8$ and $S = 2$. This value is probably overestimated due to the non-intervention of the ZFS of the Fe^{2+} but confirms the weak magnetic interactions in our compound.

Furthermore, it is interesting to examine the different possibilities of antiferromagnetic interaction among adjacent iron ions in the derived crystal structure. The minimum estimated through-bond $\text{Fe}^{\text{II}}\text{--Fe}^{\text{II}}$ distance *via* N--C--Mo--C--N bridges is 10.6155 \AA , with a Fe--Mo--Fe bond angle of 160.8° . This distance is quite large. Any meaningful through-space spin interaction between Fe^{2+} ions appears also unlikely in view of the large through space $\text{Fe}^{\text{II}}\text{--Fe}^{\text{II}}$ distances, the shortest being: $\text{Fe1} \cdots \text{Fe1}$ at 6.0394 \AA (see Table 2). Interestingly, the through-bond $\text{Fe}^{\text{II}}\text{--Fe}^{\text{II}}$ distance in this compound happens to be of the same order as in the well known Prussian Blue $\text{Fe}_4^{\text{III}}[\text{Fe}^{\text{II}}(\text{CN})_6]_3 \cdot 15\text{H}_2\text{O}$, where a long range ferromagnetic order is observed below 5.6 K (with $\theta = +6.74 \text{ K}$),¹⁸ which is attributed to a rather long $\text{Fe}^{\text{III}} \cdots \text{Fe}^{\text{III}}$ distance of 10.5 \AA across the diamagnetic $\text{Fe}^{\text{III}}\text{--N--C--Fe}^{\text{II}}\text{--C--N--Fe}^{\text{III}}$ bridges. Mayoh and Day²⁰ proposed a mechanism involving an intervalence charge-transfer configuration to explain the ferromagnetic exchange between the paramagnetic Fe^{3+} centers in

Prussian Blue. Therefore, it is interesting to compare the magnetic properties of the two compounds. The optical spectra of $[\text{Fe}_2(\text{H}_2\text{O})_4][\text{Mo}(\text{CN})_8] \cdot 4\text{H}_2\text{O}$ do not show any features other than those assigned to Fe^{2+} and $\text{Mo}(\text{CN})_8^{4-}$ components, confirming the absence of an intervalence charge transfer band. Hence, the $\text{N--C--Mo}^{\text{IV}}\text{--C--N}$ bridge can be presumed to behave as a diamagnetic linker, favoring an antiferromagnetic interaction at low temperatures.²¹ The lack of adequate through-bond interaction between Fe^{2+} spins in $[\text{Fe}_2(\text{H}_2\text{O})_4][\text{Mo}(\text{CN})_8] \cdot 4\text{H}_2\text{O}$ possibly arises from the 4d character of the Mo^{IV} , leading to a small θ value.

We were additionally interested in the photomagnetic properties of $[\text{Fe}_2(\text{H}_2\text{O})_4][\text{Mo}(\text{CN})_8] \cdot 4\text{H}_2\text{O}$ since $\text{Mo}^{\text{IV}}(\text{CN})_8^{4-}$ is a photosensitive unit exhibiting a change in its oxidation state when irradiated in the near-UV range.²² Therefore, we made an attempt to analysis the photomagnetic response of crystals of the octacyanide phase $[\text{Fe}_2(\text{H}_2\text{O})_4][\text{Mo}(\text{CN})_8] \cdot 4\text{H}_2\text{O}$. The experiment was performed at 10 K with a laser light directed through an optical fiber into the SQUID cavity where the crystal was located. The sample showed no perceptible change in its magnetic behavior after being irradiated continuously in the UV ($337 < \lambda < 356 \text{ nm}$) for several hours. It is worth mentioning that a similar experiment when conducted on a related compound $\text{Cu}_2[\text{Mo}(\text{CN})_8] \cdot 8\text{H}_2\text{O}$ did show positive results, with photoinduced magnetic interactions between adjacent spins at 10 K .¹⁹

Concluding remarks

The reaction of Fe^{2+} with molybdenum cyanides $[\text{Mo}^{\text{III}}(\text{CN})_7]^{4-}$ and $[\text{Mo}^{\text{IV}}(\text{CN})_8]^{4-}$ afforded two compounds of formula $\text{Fe}_2[\text{Mo}^{\text{III}}(\text{CN})_7] \cdot 8\text{H}_2\text{O}$ and $[\text{Fe}_2(\text{H}_2\text{O})_4][\text{Mo}^{\text{IV}}(\text{CN})_8] \cdot 4\text{H}_2\text{O}$, respectively. We have extended our previous works on $[\text{Mo}^{\text{III}}(\text{CN})_7]^{4-}$ chemistry by replacing the metal ion Mn^{2+} with Fe^{2+} . Even though the structure of $\text{Fe}_2[\text{Mo}(\text{CN})_7] \cdot 8\text{H}_2\text{O}$ is still unknown, we showed that the $\text{Mo}^{\text{III}}(\text{CN})_7^{4-}$ precursor is an efficient building block for obtaining bimetallic magnetic materials with moderate values of T_c . A three-dimensional network with the $[\text{Mo}^{\text{IV}}(\text{CN})_8]^{4-}$ precursor has structurally been characterised. The magnetic properties are essentially governed by weak antiferromagnetic interactions through diamagnetic $\text{N--C--Mo}^{\text{IV}}\text{--C--N}$ bridges. We are now studying the photomagnetic response of other similar extended systems based on $[\text{Mo}^{\text{IV}}(\text{CN})_8]^{4-}$ and hope to report in the near future some interesting results.

Acknowledgements

A. K. S. and J. V. Y. are thankful to C. E. F. I. P. R. A., New Delhi for financial support under the joint Indo-French project no. 1308-4.

References

- W. R. Entley and G. S. Girolami, *Science*, 1995, **268**, 397; S. Ferlay, T. Mallah, R. Ouahes, P. Veillet and M. Verdaguer, *Nature (London)*, 1995, **378**, 701.
- D. Babel, *Comments Inorg. Chem.*, 1982, 285; M. Verdaguer, A. Bleuzen, V. Marvaud, J. Vaissermann, M. Seuleiman, C. Desplanches, A. Scuiller, C. Train, R. Garde, G. Gelly, C. Lomenech, I. Rosenman, P. Veillet, C. Cartier and F. Villain, *Coord. Chem. Rev.*, 1999, **190–192**, 1023 and references therein.
- A. Ludi and H. Güdel, *Struct. Bonding (Berlin)*, 1973, **14**, 1.
- G. R. Rossman, F. D. Tsay and H. B. Gray, *Inorg. Chem.*, 1973, **12**, 4; M. B. Hursthouse, K. M. A. Majik, A. M. Soares, J. F. Gibson and W. P. Griffith, *Inorg. Chim. Acta*, 1980, **45**, L81; R. C. Young, *J. Am. Chem. Soc.*, 1932, **54**, 1402; J. P. Leibold, L. C. Bok and P. J. Cilliers, *Z. Anorg. Allg. Chem.*, 1974, **409**, 343.
- J. Larionova, J. Sanchiz, S. Golhen, L. Ouahab and O. Kahn, *Chem. Commun.*, 1998, 953.

- 6 J. Larionova, R. Clerac, J. Sanchiz, O. Kahn, S. Golhen and L. Ouahab, *J. Am. Chem. Soc.*, 1998, **120**, 13088; J. Larionova, O. Kahn, S. Gohlen, L. Ouahab and R. Clerac, *Inorg. Chem.*, 1999, **38**, 3621.
- 7 J. Larionova, O. Kahn, S. Golhen, L. Ouahab and R. Clerac, *J. Am. Chem. Soc.*, 1999, **121**, 3349.
- 8 O. Kahn, J. Larionova and L. Ouahab, *Chem. Commun.*, 1999, 945.
- 9 A. K. Sra, M. Andruh, O. Kahn, S. Golhen, L. Ouahab and J. V. Yakhmi, *Angew. Chem., Int. Ed.*, 1999, **38**, 2606.
- 10 G. F. McKnight and G. P. Haight, Jr., *Inorg. Chem.*, 1973, **12**, 3007.
- 11 MOLEN, Enraf-Nonius, Delft, 1990.
- 12 A. C. T. North, D. C. Philips and F. S. Mathews, *Acta Crystallogr. Sect. A*, 1968, **24**, 351.
- 13 *International Tables for X-Ray Crystallography*, ed. A. J. C. Wilson, Kluwer Academic Publishers, Dordrecht, The Netherlands, 1992, vol. C.
- 14 G. M. Sheldrick, SHELXL 97, Program for the Refinement of Crystal Structures, University of Göttingen, 1997.
- 15 J. Larionova, Thèse de l'Université de Bordeaux-1, 1998.
- 16 G. Rombaut, S. Gohlen, L. Ouahab, C. Mathonière and O. Kahn, *J. Chem. Soc., Dalton Trans.*, 2000, 3609.
- 17 W. Meske and D. Babel, *Z. Anorg. Allg. Chem.*, 1999, **625**, 51.
- 18 H. J. Buser, A. Ludi, P. Fisher, T. Studach and B. W. Dale, *Z. Phys. Chem.*, 1974, **92**, 354; A. Ito, M. Suegana and K. Ono, *J. Chem. Phys.*, 1968, **48**, 3597.
- 19 G. Rombaut, M. Verelst, S. Golhen, L. Ouahab and C. Mathonière. Unpublished results.
- 20 B. Mayoh and P. Day, *J. Chem. Soc., Dalton Trans.*, 1976, 1483.
- 21 O. Kahn, *Molecular Magnetism*, VCH, New York, 1993.
- 22 M. Shirom and Y. Siderer, *J. Chem. Phys.*, 1973, 1250; A. Vogler, W. Loose and H. Kunkely, *J. Chem. Soc., Chem. Commun.*, 1979, 187; W. L. Waltz and A. W. Adamson, *J. Phys. Chem.*, 1969, 4250.